Mapping domain disorder in exchange-biased magnetic multilayers

C. H. Marrows,[1,*] S. Langridge,[2] M. Ali,[1] A. T. Hindmarch,[1] D. T. Dekadjevi,[1,†] S. Foster,[2] and B. J. Hickey[1]
[1]*Department of Physics and Astronomy, E. C. Stoner Laboratory, University of Leeds, Leeds LS2 9JT, United Kingdom*
[2]*ISIS Facility, Rutherford Appleton Laboratory, Chilton, Didcot, Oxon OX11 0QX, United Kingdom*
(Received 24 April 2001; revised manuscript received 28 January 2002; published 30 July 2002)

Exchange anisotropy occurs at the interface between an antiferromagnetic (AF) layer and a ferromagnetic layer, and results in a ferromagnet hysteresis loop displaced along the field axis. We have performed off-specular neutron reflectometry in order to characterize the domain structure in Co layers that are exchange biased by FeMn. This allows us to determine the domain direction distributions and lateral magnetic correlation lengths for the Co layers as a function of field with the exchange bias in two different thermally prepared states: high field cooled and zero field cooled. We find that a reversing exchange-biased layer is characterized by a very short (submicron) magnetic lengthscale, indicating domains much smaller than those in the ferromagnet after ac demagnetization at temperatures above the blocking temperature. This indicates that the bias is not spatially uniform across the entire interface, underlining the complexity of the AF spin structure.

DOI: 10.1103/PhysRevB.66.024437 PACS number(s): 75.70.−i, 75.60.−d, 61.12.Ha

In general, magnetic anisotropies show rotational symmetry of an even order, as required by time-reversal symmetry. An exception is the exchange anisotropy first discovered by Meiklejohn and Bean.[1] This is observed when a ferromagnetic (FM) layer and an antiferromagnetic (AF) layer are brought into atomic proximity, so that there are exchange interactions between the planes of spins on either side of the interface. The most commonly reported manifestation of this exchange interaction is a shift in the hysteresis loop of the ferromagnetic layer, which can be interpreted as a unidirectional anisotropy. This is commonly characterized by an exchange field H_{ex}, the field through which the center of the hysteresis loop of the ferromagnet is shifted from zero. This loop shift leads to the term ''exchange bias,'' and is of technological importance in the design of thin-film magnetic devices.[2,3] While over four decades have elapsed since Meiklejohn and Bean's discovery, a rigorous description of the phenomenon is still lacking.[4–6] One particular problem has been the issue of the low value of H_{ex} compared to what might naïvely be anticipated.

One approach to reducing the H_{ex} to a level more commensurate with that generally obtained by experiment is to consider, in a more realistic manner, the defects that will occur at the interface in real materials. These will lead to a random field that breaks the antiferromagnetic film into domains over its area, with walls forming perpendicular to the interface.[7] This idea has recently been extended to a bulk random field, giving volume antiferromagnetic domains, caused by vacancies and defects in the antiferromagnetic film.[8] This type of approach has been pursued as an explanation for the enhancement in coercivity that commonly accompanies the shift in the hysteresis loop.[9] Recently some experimental progress has been made in attempting to confirm these theoretical ideas.[10,11] A major barrier to progress has been the experimental challenge of imaging the domain structure of an antiferromagnet, recently accomplished in the case of $LaFeO_3$ by Nolting *et al.*[12] and NiO by Stöhr *et al.*[13] using x-ray magnetic dichroism coupled with photoemission electron microscopy. However, such methods are ineffective in the commonly used family of Mn alloys due to the lack of a strong dichroism signal in these metallic materials. An alternative to direct imaging is a scattering approach using magnetically sensitive radiation, such as neutron diffraction.[14] In this paper we examine the reversal mechanisms of biased FM layers after cooling the AF/FM system through the AF ordering temperature, having prepared a suitable domain state in the FM layer. We are able to determine a number of important statistical variables relating to the domain structure in the FM layer through the use of off-specular neutron reflectometry.[15] We then correlate different domain structures with changes in the exchange bias properties.

We have chosen the FeMn/Co system for our studies, as the blocking temperature (the temperature above which the exchange bias vanishes) of the FeMn is 150 °C, which is substantially lower than the Curie point T_{C} of the Co. This ensures that we can maintain strong FM ordering within the Co layers, while completely disordering the FeMn at a temperature that is easily accessed experimentally, and without significantly altering the film properties due to high temperature annealing.

Our films were prepared by dc magnetron sputter deposition in a custom built vacuum system with a base pressure $\sim 2\times10^{-8}$ Torr. The working gas was Ar at a pressure of 3.0 mTorr, and deposition rates were typically 2.5 Å/s. A 200-Oe field was applied in the sample plane during deposition. Nominal film thicknesses were confirmed by x-ray reflectometry. Magnetization loops were measured by the magneto-optic Kerr effect (MOKE) with the sample mounted on a heater stage allowing the temperature to be raised up to 250 °C. Our sputtered samples are polycrystalline, with a weak (111) texture, but with no preferred crystallographic direction in the plane. We therefore chose the direction of the growth field as the direction in which to apply fields during the various experiments.

The neutron reflectometry was carried out using the CRISP instrument at the ISIS spallation source.[16] Specular reflectivity profiles were measured with the incident neutron beam polarized. The incident beam polarization was greater than 95% over the wavelength range used, and all the data we show are corrected for polarizer and flipper efficiencies.

The figure legend refers to the spin eigenstate of the incident neutron flux. In this case the instrument resolution $\Delta Q_Z/Q_Z$ is $\sim 4\%$. More importantly in this paper, by combining the time-of-flight technique with a one-dimensional (1D) multidetector we were able to capture in parallel, an entire reciprocal space map from the sample, requiring typically 2 h to acquire good statistics. The resolution in Q_X is $\sim 3 \times 10^{-5}$ Å^{-1}. In this case the instrument was run in unpolarized mode in order to maximize the available neutron flux at the sample, which will decrease counting times as well as lowering the noise floor of the instrument. In both cases the sample is placed between the poles of an electromagnet on a second similar heater stage, allowing the exchange-bias properties to be reset within the reflectometer.

The neutron scattering data allows us to extract statistical quantities, characterizing the micromagnetic state of the entire sample using our previously published model.[15] Although the model is not fully dynamical,[17] it is still possible to capture much of the essential physics within a kinematic formalism.[18] Since the momentum-transfer vector has components both in the sample plane and perpendicular to it, we are able to obtain magnetic correlation lengths (ξ) in both the *X* and *Z* directions. The in-plane coherence length of the neutron beam is some tens of μm, so that we are easily able to extract reliable data on domains of the order of μm size or smaller. We are also able to determine the width of the angular distribution of domain directions in the plane of the sample, σ. Here *X* is in the sample plane, while *Z* is parallel to the film normal; these two axes span the plane containing the incident and specular outgoing beams. The field is applied parallel to the *Y* axis, and intensity variations in this direction are integrated out in our 1D detector geometry.

Although we investigated a number of samples, we shall concentrate our attention in this paper on one representative multilayer of the form Si/Ta (75 Å)/FeMn (100 Å)/{Co (50 Å)/FeMn (100 Å)}×10/Ta (50 Å). Although FM/AF bilayers are most commonly investigated in studies of exchange bias, the use of multilayer geometry leads to Bragg peaks in the neutron reflectometry data, maximizing the information available from this technique. In Fig. 1, the MOKE hysteresis loop and specular polarized neutron reflectivity spectra at selected values of the applied field are shown for the as-grown sample. From the Kerr loop it is immediately evident that the growth field has induced an exchange bias in the Co layers, with a hysteresis loop offset of 130 Oe.

Considering the neutron reflectivity curves in Fig. 1, we can see that there is a strong multilayer Bragg peak at a perpendicular momentum transfer vector Q_Z of 0.042 Å^{-1}, corresponding to a real space periodicity of 150 Å which is in good agreement with the x-ray thickness measurements. Note that when the sample is in a state close to saturation [panels (b) or (e)], there is a splitting in the Q_Z positions of the spin-↑ and spin-↓ Bragg peaks corresponding to dynamical effects at low *Q*—different effective refractive indices for the magnetized multilayer for neutrons of different spin. The observation of this splitting was previously taken to indicate that the sample is close to a single-domain configuration.[19] This is in addition to the intensity splitting that reveals a net moment along the field axis. Note that the reversal of the saturated magnetization of the sample leads to a switching of the spectra for the two spin channels at the Bragg peak and critical edge. Note that our discussion here pertains only to the ferromagnetic Co layers. In this *Q* range the neutrons have no sensitivity to the antiferromagnetism of the FeMn layers; our experiment is only sensitive to magnetism through the total induction **B** within the sample in reflectometry experiments, which depends on the magnetization of the Co layers. In panel (e) the critical edge for spin-↓ neutrons is just below the *Q* range over which we have collected data.

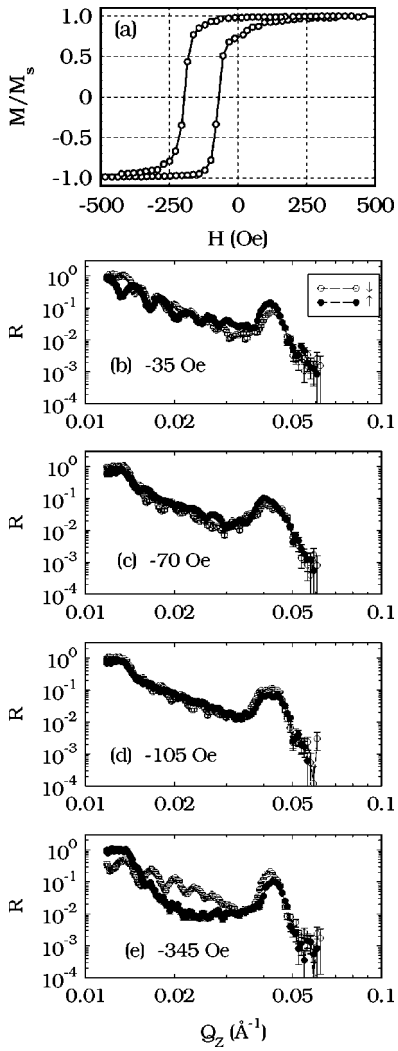

FIG. 1. (a) Kerr loop of the as-grown FeMn/Co multilayer at room temperature. (b)–(e) Polarized neutron reflectivity spectra for the as-grown FeMn/Co multilayer at various applied fields of interest on the positive-going branch of the hysteresis loop.

The Bragg peaks show an interesting field dependence. The width of the Bragg peaks in Q_Z indicates a vertical coherence length $\xi_Z = 2\pi/\Delta Q_Z$ of ~ 1100 Å for the narrower peaks observed before and after switching at -35 and -345 Oe [panels (b) and (e)]. This length scale is comparable with the entire stack height of the multilayer. The peaks are much broader during switching at -70 and -105 Oe [panels (c) and (d)], apparently giving a reduced ξ_Z of

$\sim$800 Å. Note, however, that the broadening of the peaks is asymmetric—each peak broadens towards its spin-split neighbor, and they exchange places when comparing the spectra prior to and after magnetic switching. Although there appears to be some loss of vertical coherence, a substantial part of the broadening is due to a superposition of peaks at the two possible Bragg positions corresponding to the two spin channels, and the true value of ξ_Z during reversal will actually be somewhat longer than the 800 Å given above. It is not a trivial process to deconvolute these two effects.

We have also performed a reciprocal-space mapping of the scattered intensity from the sample in this state in order to determine the form of the diffuse neutron scatter. In Fig. 2 we show typical reciprocal space maps for our sample. First- ($Q_Z = 0.042$ Å^{-1}) and second- ($Q_Z = 0.084$ Å^{-1}) Bragg peaks are clearly visible along the specular ridge ($Q_X = 0$). In Fig. 2(b), where the applied field is in the midst of causing magnetic reversal, we see a considerable amount of diffusely scattered neutrons. This off-specular intensity does not appear solely around the Q_Z value of the Bragg peak, as we previously observed in multilayers with a highly vertically coherent magnetic microstructure.[20] Instead we see diffuse intensity distributed throughout those areas of reciprocal space in the vicinity of the specular ridge. In an x-ray characterization of multilayers, such diffuse intensity is associated with interfacial roughness that is uncorrelated from one interface to the next.[21] In this case, because of the field dependence, it can be ascribed to some loss of vertically coherent magnetic domains in the Co layers. It is possible to discern a Yoneda feature highlighted by this additional intensity for negative Q_X—visible only on one side of the specular ridge due to the time-of-flight geometry of the measurement.[22] This can be seen as a line of scattered intensity with constant Q_X/Q_Z just within the kinematic limits of the experiment in the lower left corner of panel (b), marked with a dashed white line. It is possible that the study of such ''magnetic'' Yoneda-type features may yield additional information on the magnetic domain distribution and/or the magnetic roughness.[23]

After heating our sample to 200 °C we find that we have lost all exchange bias properties and recover the intrinsic properties of the Co layers, and the loop is no longer shifted. As we can see in Fig. 3, the loop is centered about zero field and the coercive field is now only $\sim$20 Oe. As the blocking temperature in FeMn films is generally found to be 150 °C this is unsurprising—we are at a temperature where the FeMn is magnetically disordered. Again we obtain sharp Bragg peaks in both Q_Z and Q_X when the film is in a saturated state, but there is an appreciable diffuse background due to uncorrelated magnetic domain structures at the coercive field.

By taking a section along Q_X through the reciprocal space map of the heated samples, we are able to quantify the angular domain spread σ and lateral magnetic coherence length ξ_X, as we did in the past for antiferromagnetically coupled multilayers.[15] At a saturating field of 500 Oe we find that, upon performing such a sectioning, we observe a specular ridge without any diffuse scatter, shown in Fig. 4(b). Therefore, any diffuse scattering caused by structural roughness in our sample is below the resolution of our measurement. At this point it should be noted that in our modeling and fitting, the simulated intensity profile is convoluted with an instrument function in order to accurately reflect the limited instrumental resolution in our experiments. However, during the magnetic switching process the diffuse background is easily observed and fitted by our model, as can be seen in Fig. 4(a). These sections, and all further Q_X sections that we show, were acquired at a smaller incident angle for the neutron beam than in Fig. 2, placing the first-order Bragg peak more centrally in the region of reciprocal space we have probed. This means that we have increased the limits on Q_X and so the scans extend further in the positive Q_X direction. For these fits we obtain $\sigma = 0.29$ rad and $\xi_X = 1.9$ μm at the coercive field of -20 Oe, while in the saturating field of -500 Oe we set $\sigma = 0$, leading to an effectively infinite ξ_X. The only contribution to the diffuse scatter we include is a structural roughness of $\sim$2 Å, a low level and difficult to discern with our instrumental resolution. This level of structural roughness is then included in all other fits. As before,[15] we interpret these lengths ξ_X as being characteristic of the lateral magnetic domain size. The Yoneda feature is clearly visible in the scatter for negative Q_X. As our model for the diffuse magnetic scattering makes use of the Born approximation we are unable to treat these dynamical effects at present. Nevertheless it can be seen that otherwise a good fit to the data is achieved.

We now turn to the preparation of the sample in different ''frozen-in'' domain configurations. After exploring the high-temperature regime, we cooled the sample back to room temperature in a field well in excess of that needed to saturate the Co layers, 3300 Oe. In Fig. 5 we show the Kerr loop for the sample after this process. It appears similar to the as-grown loop, although the bias field has risen to 175 Oe after this process. The switching of the layers is relatively sharp, with transition widths of $\sim$50 Oe in the forward and reverse directions. The sample is close to positive saturation when brought to zero field from either direction.

The neutron results from the sample in the field-cooled state are qualitatively very similar to those in the as-grown state. Diffuse scatter arises at no particular Q_Z value in reciprocal space, indicating weakly correlated switching in the different Co layers. We have mapped the scatter and fit to Q_X sections through the Bragg peak for several fields as the sample reverses magnetically, shown in Fig. 6. The small asymmetry in Q_X observable arises from the proximity of the transmitted beam for $-Q_X$. We show the domain spread σ and lateral correlation length ξ_X as functions of the field in Fig. 7. We are unable to make meaningful quantitative measurements of σ and ξ_X when the sample is close to saturation, due to the very low level of diffuse scatter, which makes the fitting unreliable at these fields. However, we are able to gain an insight into the evolution of the domain processes within the switching field window.

First, examining the behavior of σ in Fig. 7(a), we can see that this variable peaks at -240 Oe for the negative-going data and -100 Oe for the positive-going data. These closely match the coercive fields determined from the Kerr loop in Fig. 5. Hence, as perhaps might be anticipated, the domain

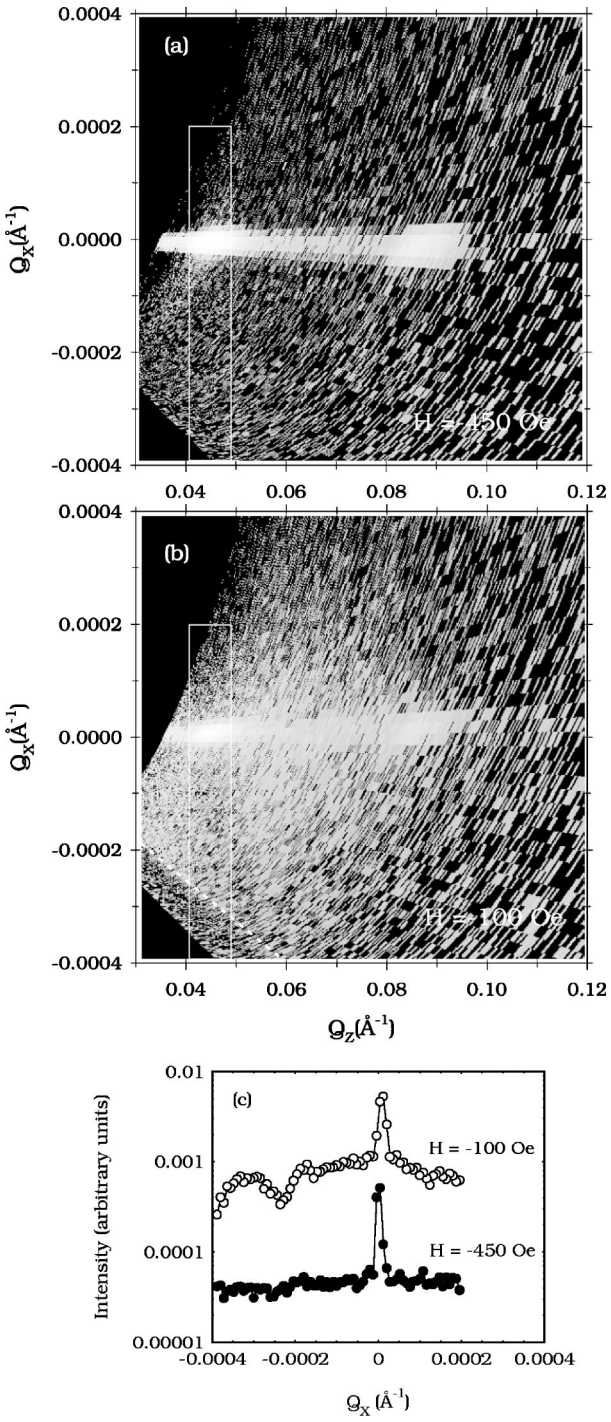

FIG. 2. Reciprocal space maps of the FeMn/Co multilayer sample in the as-grown state in (a) a saturating field and (b) the coercive field. Both first- and second-order Bragg peaks are visible along the specular ridge. The dark areas represent regions of reciprocal space beyond the kinematical limits of the experiment (Ref. 24). The ridge of scattered intensity at a constant exit angle, marked with a dashed line in panel (b), is the Yoneda feature. Panel (c) shows the Q_X sections through the first-order Bragg peak. The cutoff at positive Q_X is due to the limits of the area of reciprocal space probed: we have integrated in Q_Z the data within the white boxes in panels (a) (solid markers) and (b) (open markers) to yield the sections shown.

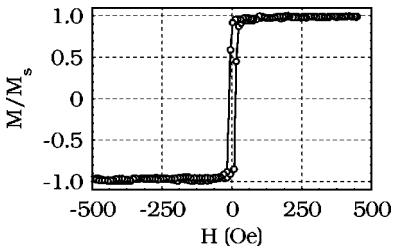

FIG. 3. Kerr loop of the FeMn/Co multilayer when heated to 200 °C, above the blocking temperature of the FeMn.

population is most disordered at the coercive field. However the peak value of σ is higher in the positive-going data. Asymmetric reversal mechanisms have been reported previously,[25] where an Fe/MnF_2 bilayer was found to reverse by coherent rotation or domain propagation on different sides of the hysteresis loop. We can explain the higher peak for σ in the positive-going data as being due to a higher proportion of the reversal occurring by domain propagation when the field is swept in this direction. Coming now to examine the size of these domains in panel (b), the most striking feature is the very small values of ξ_X. As the field is reversed against the pinning direction, the Co layers break into domains with a typical size of ~ 1.5 μm. As the layer reverses these domains shrink until they are smaller than 1 μm, before reversal completes, where we will again have a single reversed domain. It is noteworthy that ξ_X is much smaller here than it ever was at 200 °C, when the Co layers were unbiased. Panel (c) shows the integrated intensity I_0 for the diffuse scatter—this peaks at the coercive fields and shows a similar qualitative form to the σ data in panel (a). The hysteresis easily seen in $\sigma(H)$ and $I_0(H)$ is hard to discern in $\xi_X(H)$. This indicates a greater degree of reversal by rotation on the positive-going field sweep, although the typical domain size is comparable in both branches.

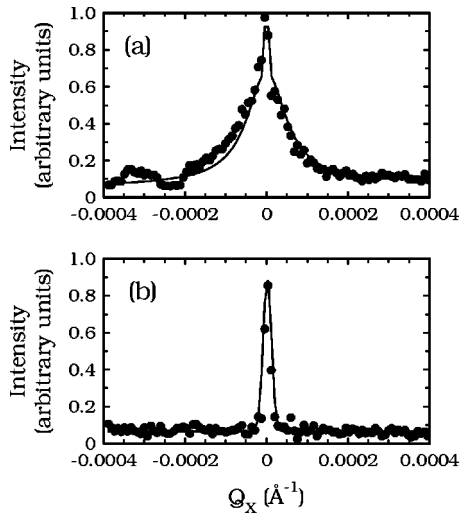

FIG. 4. Sections through the Bragg peak ($Q_Z = 0.042$ Å^{-1}) in Q_X at a temperature of 200 °C. The circles represent experimental data, while the lines are fits from the model. (a) $H = -20$ Oe (coercive field). (b) $H = -500$ Oe (saturating field). Note that the Yoneda feature can be observed in the scatter at negative Q_X in panel (a).

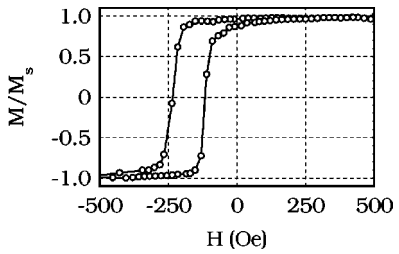

FIG. 5. Kerr loop of the FeMn/Co multilayer after cooling from 200 °C to room temperature in a 3300-Oe field.

The breakup of an exchange-biased ferromagnetic layer into very small, irregular domains was previously observed in the IrMn/Co system using field-dependent magnetic force microscopy.[26] The domain size was found to be significantly smaller in the exchange-biased films than in unbiased Co films. Similar results were found by Lorentz transmission electron microscopy when imaging IrMn biased films of permalloy—reversal was characterized by sub-micron domains of irregular form,[27] which were not observed above the blocking temperature. The very short ξ_X lengths that we observe, corresponding to the very extended scatter in Q_X, are therefore consistent with the results of these direct imaging techniques. Moreover it is also interesting to compare the asymmetric behavior of ξ_X with imaging techniques as well. We can only observe off-specular neutron scatter when there is a domain structure in the sample, due to the low structural and magnetic roughness. Nevertheless, it is possible to draw some conclusions about the nucleation process. During reversal against the pinning the initial domains are large, suggesting few nucleation sites. The opposite is true during return to the pinned state—the small domains must have many nucleation sites. Similar nucleation processes were observed by the magneto-optic indicator film (MOIF) technique in a NiO/NiFe bilayer.[28]

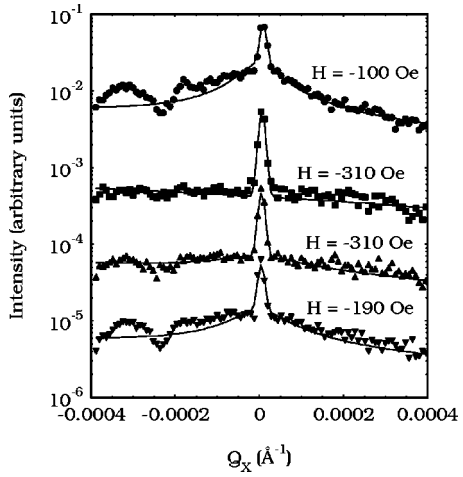

FIG. 6. Sections through the Bragg peak ($Q_Z = 0.042$ Å^{-1}) in Q_X for various applied fields at room temperature, after cooling from 200 °C to room temperature in a 3300-Oe field. All data are on the positive-going field branch but for the solid squares, which are on the negative-going branch of the hysteresis loop. The solid lines are fits from the model.

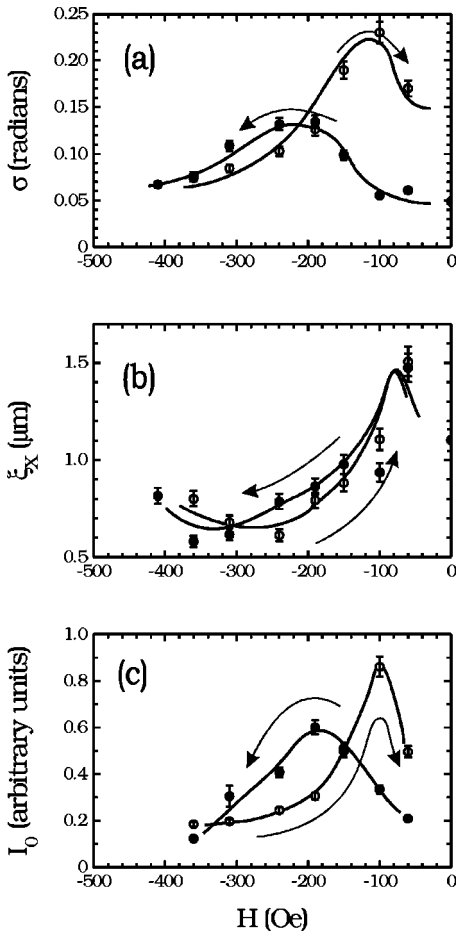

FIG. 7. Field dependence of (a) the domain distribution width σ, and (b) the lateral magnetic correlation length ξ_X, as determined by fitting to diffuse neutron scatter, after cooling from 200 °C to room temperature in a 3300-Oe field. Panel (c) shows the field dependence of the integrated diffuse intensity at the first order Bragg peak ($Q_Z = 0.042$ Å^{-1}). The solid lines are guides to the eye, and the arrows indicate the direction of the field sweep.

In our second domain cooling experiment the sample was heated to 200 °C and then ac demagnetized. The remanent field of the electromagnet pole pieces was then nulled off with a small reverse current so that the field at the sample was <1 Oe, before cooling back to room temperature. The Kerr loop we obtained after carrying out such a process in our laboratory is displayed in Fig. 8. It is completely differ-

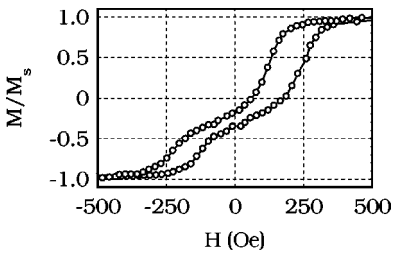

FIG. 8. Kerr loop of the FeMn/Co multilayer after cooling from 200 °C to room temperature in zero field following ac demagnetization.

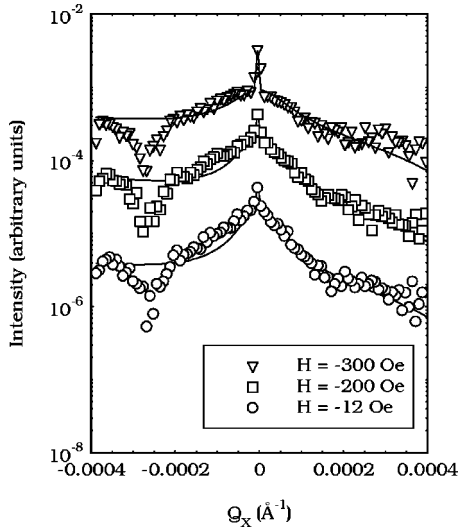

FIG. 9. Sections through the Bragg peak ($Q_Z = 0.042$ Å^{-1}) in Q_X for various applied fields at room temperature, after cooling from 200 °C to room temperature in zero field following ac demagnetization. The solid lines are fits from the model.

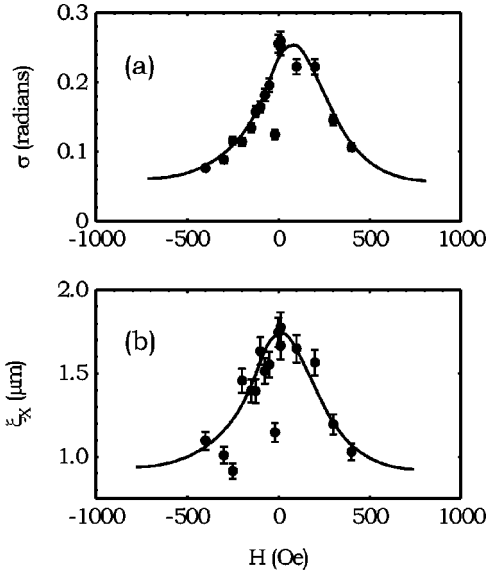

FIG. 10. Field dependence of the domain distribution width σ and lateral magnetic correlation length ξ_X in the ac-demagnetized/zero-field-cooled state as determined by fitting to diffuse neutron scatter. The solid lines are guides to the eye.

ent in character to all the other loops we have shown. The magnetization is continuously reversing throughout the loop, with a pronounced kink around zero field. Indeed, the loop has the appearance of various sections of the layers being biased in different directions—although imperfections in the ac demagnetization process have left a domain population shifted rather more toward positive fields than toward negative ones, as can be seen by the fact that the loop crosses the ordinate with negative values of M/M_s for both branches of the curve. However the field scales are rather symmetric: the loop saturates at ~ 350 Oe in both directions, and the bias and coercive fields of the domains pinned in either direction are rather similar. Hysteresis loops of this form were observed by Gökemeijer *et al.* after such a field-cooling procedure.[29]

This loop is consistent with the idea of a transfer of a complex domain pattern to the FeMn layers (with a small weighting to domains magnetized in the negative direction), so that each domain in the Co is locally pinned in the direction it took up during cooling. Application of positive or negative fields causes those areas pinned in the opposite direction to be reversed, leading to the wasp-waisted loop observed in Fig. 8. Analyzing the diffuse neutron scatter in the remanent state (Fig. 9) we obtain a domain spread, σ, of ~ 0.26 rad, and an in-plane correlation length ξ_X of 1.8 μm. Evidently, the domains in the Co are of comparable size after the ac demagnetization process and at the coercive field during a quasistatic dc hysteresis loop at 200 °C, as seen in Fig. 3. The domain spread seems rather small, and this might be due to limitations in our model, where a Gaussian distribution of domain directions with a width smaller than 2π rad is assumed.[15] As we have already suggested that the domain distribution after ac demagnetization contains domains that are exchange biased in many directions, it seems unlikely that this is realistic. Such distributions have been directly observed by Scholl *et al.*[30] (Note that this problem does not affect the reliability of the values we obtain for ξ_X, as it is determined essentially from the reciprocal of the half-width of the Bragg peak when sectioned along Q_X.) Nevertheless we can see that the trend in σ with field in Fig. 10 is as expected, with the domains focusing around the applied field direction as that field is made stronger. It is difficult to observe much by way of hysteresis in these data, with the points clustered around the lines representing the general trend.

Meanwhile, we observe a decrease in ξ_X with strengthening field of either sense, shown in Fig. 10, initially counterintuitive and contrary to previously reported findings.[15] However, recalling the field dependence of ξ_X in the case of the field-cooled multilayer, an explanation is at hand. There it was found that an exchange-biased bilayer will break up into many small domains during reversal against the pinned direction. The shortening of ξ_X into the submicron regime with applied field is therefore to be associated with the reversal of those areas of the Co layers which are biased against the direction in which the field is decreasing. Again, once reversal is complete, these very small domains annihilate and the diffuse neutron scatter to which we can fit is lost.

We can draw two main conclusions from a consideration of these results. The observation that the reversal of the exchange biased ferromagnetic layers proceeds by a disruption of the magnetization into a domain state with a much shorter lateral coherence length than anything observed in similar unbiased films leads us to conclude that the spin structure of the antiferromagnetic interface layers can be spatially uniform on, at most, short sub-micron lengthscales. Therefore single domain models of exchange bias[31–34] can hope to describe exchange bias at best only locally.

Second, noting that the Co layers broke into these small domains even when the sample was field cooled in a single-domain state, we can see that this nonuniform AF spin struc-

ture is induced by some other influence. This process has been described by Malozemoff[7] as being due to a randomness in the exchange interactions at the interface between the AF and FM layers, which breaks the AF material into domains due to local imbalances in the number of uncompensated spins at the interface.[35] On the other hand, the calculations of Nowak *et al.*[8] described the possibility for this to occur in the volume of the AF film if there are bulk defects such as vacancies or impurity atoms that can lead to similar statistical imbalances in the number of spins, so that it is the cooling field itself that sets up the AF domain structure. This mechanism seems to contribute only a small part of the bias in our samples, however—we cooled a sample in zero field after dc demagnetizing in our Kerr apparatus and still measured a bias as large as seen in the as-grown (Fig. 1) or field-cooled states (Fig. 5). Close examination of the high temperature hysteresis loop in Fig. 3 shows that the squareness of the loop is very high, so that the sample is still close to a single-domain state during cooling. It is therefore the coupling to the Co layers at the interface that determines the AF domain structure.

It is important to consider what information about the AF domain structure we can glean from the data available from these experiments. We find that when the FeMn is in an ordered state it reduces the domain size in the Co during reversal significantly. Therefore, from the measurements of ξ_X that we have obtained we can set an upper limit for the characteristic size of the domains in the AF layers as roughly the minimum value for ξ_X that we obtain, *viz.* slightly less than 1 μm. It is likely that it is in fact smaller than this length scale, as the strongly coupled nature of the ferromagnetic film will tend to smear out fine disorder, in much the same way that occurs in the production of only a gentle magnetic ripple from randomly oriented anisotropy axes in small grains.[36,37] It is worth remarking that the correspondence between the AF and FM domains in the work of Nolting *et al.* was striking.[12]

The description of the domain structure in the ac demagnetized, zero-field-cooled sample requires a second level of sophistication. After ac demagnetization we obtain a value for ξ_X of ~ 2 μm, a length scale which is then frozen in upon cooling back to room temperature. This represents the ''natural'' size of the domains in the Co layers. Each of these regions of 2-μm size is magnetized uniformly in a specific direction, and therefore induces an overall imbalance of AF interface spins upon cooling across that area. However, we can see from the data presented in Fig. 10 that the AF layer must still be highly spatially nonuniform within these regions so that the local spin imbalance is aligned with underlying magnetization of the FM layers. These small domains are of a similar size to those seen in the field-cooled sample. Hence it is reasonable to regard each area defined by a FM domain as having the same properties as if it had been field cooled with the field applied parallel to that domain's magnetization. We can see that locally the exchange bias has the same magnitude as in the field-cooled case, but is oriented locally according to the domain distribution found in the FM layers. The results of recently reported MOIF experiments are consistent with this interpretation.[38] The situation could be complicated somewhat in the present case by the fact that all but the outermost of our FeMn layers is in contact with two Co layers, meaning that two potentially different domain configurations must be satisfied. However, we do not observe large differences in the values of ξ_Z for the various different states of our sample—always at least 1100 Å in a ''saturated'' state, and dropping to not less than 800 Å during reversal, suggesting that the domain structures in at least a few nearby Co layers are similar.

In short, our main findings are: that preparation of different domain states in the FM prior to cooling through the blocking temperature of the AF domain leads to each FM domain being locally biased in its own direction; that during magnetization reversal very small FM domain structures are formed, indicating the formation of spatial inhomogeneities in the AF spin structure during cooling which are no larger than 1 μm; and that the reversal mechanisms on either side of the hysteresis loop are more asymmetric than might be supposed from an examination of the Kerr loops alone.

C. H. M. is grateful to the Royal Commission for the Exhibition of 1851 for financial support. We would also like to thank the Rutherford Appleton Laboratory for the provision of ISIS beamtime, and T. P. A. Hase for useful discussions.

*Email address: c.marrows@leeds.ac.uk
†Present address: Laboratorio MDM-INFM, Via Olivetti 2, I-20041 Agrate-Brianza (Mi), Italy.

[1] W. H. Meiklejohn and C. P. Bean, Phys. Rev. **102**, 1413 (1956).
[2] J. C. S. Kools, IEEE Trans. Magn. **32**, 3165 (1996).
[3] S. S. P. Parkin, K. P. Roche, M. G. Samant, P. M. Rice, R. B. Beyers, R. E. Scheuerlein, E. J. O'Sullivan, S. L. Brown, J. Bucchigano, D. W. Abraham, Y. Lu, M. Rooks, P. L. Trouilloud, R. A. Wanner, and W. J. Gallagher, J. Appl. Phys. **85**, 5828 (1999).
[4] J. Nogués and I. K. Schuller, J. Magn. Magn. Mater. **192**, 203 (1999).
[5] A. E. Berkowitz and K. Takano, J. Magn. Magn. Mater. **200**, 552 (1999).
[6] M. Kiwi, J. Magn. Magn. Mater. **234**, 584 (2001).
[7] A. P. Malozemoff, Phys. Rev. B **35**, 3679 (1987); J. Appl. Phys. **63**, 3874 (1988); Phys. Rev. B **37**, 7673 (1988).
[8] U. Nowak, A. Misra, and K. D. Usadel, J. Appl. Phys. **89**, 7269 (2001); J. Magn. Magn. Mater. **240**, 243 (2002).
[9] Z. Li and S. Zhang, Phys. Rev. B **61**, 14897 (2000); Appl. Phys. Lett. **77**, 423 (2000).
[10] P. Miltényi, M. Gierlings, J. Keller, B. Beschoten, G. Güntherodt, U. Nowak, and K. D. Usadel, Phys. Rev. Lett. **84**, 4224 (2000).
[11] K. Liu, S. M. Baker, M. Tuominen, T. P. Russell, and I. K. Schuller, Phys. Rev. B **63**, 060403 (2001).
[12] F. Nolting, A. Scholl, J. Stöhr, J. W. Seo, J. Fompeyrine, H. Siegwart, J.-P. Locquet, S. Anders, J. Lüning, E. E. Fullerton, M. F. Toney, M. R. Scheinfein, and H. A. Padmore, Nature (London)

405, 767 (2000).
[13] J. Stöhr, A. Scholl, T. J. Regan, S. Anders, J. Lüning, M. R. Scheinfein, H. A. Padmore, and R. L. White, Phys. Rev. Lett. **83**, 1862 (1999).
[14] J. A. Borchers, Y. Ijiri, D. M. Lind, P. G. Ivanov, R. W. Erwin, A. Qasba, S. H. Lee, K. V. O'Donovan, and D. C. Dender, Appl. Phys. Lett. **77**, 4187 (2000).
[15] S. Langridge, J. Schmalian, C. H. Marrows, D. T. Dekadjevi, and B. J. Hickey, Phys. Rev. Lett. **85**, 4964 (2000).
[16] R. Felici, J. Penfold, R. C. Ward, and W. G. Williams, Appl. Phys. A: Solids Surf. **45**, 169 (1988).
[17] Other groups are working on the development of a fully dynamical model, recent reports include B. P. Toperverg, Physica B **297**, 160 (2001); B. Toperverg, O. Nikonov, V. Lauter-Pasyuk, and H. J. Lauter, *ibid.* **297**, 169 (2001).
[18] S. K. Sinha, in Neutron Scattering in Materials Science, edited by D. A. Neumann, T. P. Russell, and B. J. Wuensch, MRS Symposia Proceedings No. **376** (Materials Research Society, Pittsburgh, 1995), p. 175.
[19] S. Adenwalla, G. P. Felcher, E. E. Fullerton, and S. D. Bader, Phys. Rev. B **53**, 2474 (1996).
[20] S. Langridge, J. Schmalian, C. H. Marrows, D. T. Dekadjevi, and B. J. Hickey, J. Appl. Phys. **87**, 5750 (2000).
[21] V. Holý and T. Baumbach, Phys. Rev. B **49**, 10668 (1994).
[22] The absence of a Yoneda feature for positive Q_X can be understood more easily by drawing an analogy between the time-of-flight method and the more traditional scattering geometry where the detector is scanned and monochromatic radiation is used. Our map is effectively built up from a series of detector scans where the sample is fixed with respect to the incident beam. In this case only the exit beam can make the critical angle with the surface—an example of such a detector scan performed with x rays can be found in I. Pape, T. P. A. Hase, B. K. Tanner, and M. Wormington, Physica B **53**, 278 (1998). The Yoneda feature can only be seen on one side.
[23] G. P. Felcher (private communication).
[24] See, for example, Z. X. Li, J. R. Lu, R. K. Thomas, A. Weller, J. Penfold, J. R. P. Webster, D. S. Sivia, and A. R. Rennie, Langmuir **17**, 5858 (2001).
[25] M. R. Fitzsimmons, P. Yashar, C. Leighton, I. K. Schuller, J. Nogués, C. F. Majkrzak, and J. A. Dura, Phys. Rev. Lett. **84**, 3986 (2000).
[26] J. Yu, A. D. Kent, and S. S. P. Parkin, J. Appl. Phys. **87**, 5049 (2000).
[27] J. P. King, J. N. Chapman, M. F. Gillies, and J. C. S. Kools, J. Phys. D **34**, 528 (2000).
[28] V. I. Nikitenko, V. S. Gornakov, L. M. Dedukh, Yu. P. Kabanov, A. F. Khapikov, A. J. Shapiro, R. D. Shull, A. Chaiken, and R. P. Michel, Phys. Rev. B **57**, 8111 (1998).
[29] N. J. Gökemeijer, J. W. Cai, and C. L. Chien, Phys. Rev. B **60**, 3033 (1999).
[30] A. Scholl, F. Nolting, J. Stöhr, T. Regan, J. Luning, J. W. Seo, J. P. Locquet, J. Fompeyrine, S. Anders, H. Ohldag, and H. A. Padmore, J. Appl. Phys. **89**, 7266 (2001).
[31] D. Mauri, H. C. Siegmann, P. S. Bagus, and E. Key, J. Appl. Phys. **62**, 3047 (1987).
[32] N. C. Koon, Phys. Rev. Lett. **78**, 4865 (1997).
[33] T. C. Schulthess and W. H. Butler, Phys. Rev. Lett. **81**, 4516 (1998).
[34] R. L. Stamps, J. Phys. D **33**, 247 (2000).
[35] K. Takano, R. H. Kodama, A. E. Berkowitz, W. Cao, and G. Thomas, Phys. Rev. Lett. **79**, 1130 (1997).
[36] H. Hoffmann, IEEE Trans. Magn. **4**, 32 (1968).
[37] K. J. Harte, J. Appl. Phys. **39**, 1503 (1968).
[38] R. D. Shull, A. J. Shapiro, V. S. Gornakov, V. I. Nikitenko, N. J. Gökemeijer, and C. L. Chien (unpublished).